

# Characterization of laser seeding by use of group-velocity dispersion in an atomic-vapor filter

Azer P. Yalin, Peter F. Barker, and Richard B. Miles

*Department of Mechanical and Aerospace Engineering, Princeton University, Princeton, New Jersey 08544*

Received October 1, 1999

A method for measuring laser seeding efficiencies by use of group-velocity dispersion has been developed. By tuning the laser near a resonance in an atomic-vapor filter it is possible to temporally decouple the seeded (narrow-band) light from the unseeded (broadband) light. We measured a seeding efficiency of 99.8% of the third harmonic of an injection-seeded Ti:sapphire laser. A model for the observed dispersion has been developed and tested. The group-velocity dispersion in the filter may also be used to chirp pulses for spectral analysis in the time domain. © 2000 Optical Society of America

OCIS codes: 300.6500, 190.5530, 140.3590.

A novel method for discriminating between the seeded narrow-band and the unseeded broadband components of a seeded laser has been developed and can be used to measure laser seeding efficiencies. Often laser seeding efficiencies are high, quoted as greater than 99%, making it a challenging problem to measure the small fraction of broadband light present in the beam. However, in many spectroscopic applications it is important to have accurate knowledge of the seeding efficiency, or spectral purity. For example, in measurements of laser-induced fluorescence the broadband light will interact with nonresonant transitions, and in filtered Rayleigh scattering measurements the elastic background suppression may be compromised.<sup>1</sup> To measure the small fraction of broadband light, techniques that measure the light transmission near optically thick transitions have been developed.<sup>2</sup> These methods require accurate spectral knowledge of the transition in use, of the laser frequency, and of the narrow-band linewidth. In contrast, our method uses group-velocity dispersion (GVD) to decouple the narrow-band and broadband components to permit a direct determination of the laser seeding efficiency. Seeding efficiency can be measured on a shot-to-shot basis, and precise knowledge of the laser characteristics or of the vapor characteristics is not required. To demonstrate the technique we measured the seeding efficiency of the third-harmonic output of an injection-seeded Ti:sapphire laser to be ~99.8%.

Our method uses the strong variation in group velocity near an atomic resonance to temporally separate frequency components within a pulse of width ~20 ns. Tuning the laser near a resonant transition of the vapor filter causes the seeded (narrow-band) portion of the light to propagate through the filter with a group velocity that is significantly less (of the order of 100 times) than the speed of light. The unseeded light is broad in frequency compared with the absorption bandwidth and therefore travels through the filter at close to the speed of light. Its slower group velocity means that the seeded light is delayed relative to the unseeded light, permitting temporal discrimination between the two components. Delayed pulses in rubidium vapor were observed previously<sup>3</sup>; furthermore, GVD in atomic vapors has been used to measure

Lorentzian linewidths<sup>4</sup> and to determine electric transition dipole moments.<sup>5</sup>

The GVD is due to the variation in the real part of the index of refraction<sup>6</sup>:

$$V_g(\omega) = \frac{c}{\left(n + \omega \frac{dn}{d\omega}\right)}, \quad (1)$$

where  $V_g$  is the group velocity,  $c$  is the speed of light,  $n$  is the index of refraction,  $\omega$  is the radial frequency, and  $dn/d\omega$  is the derivative of real index with respect to radial frequency. The real index of refraction near a transition is given as<sup>6</sup>

$$n = 1 - \left(\frac{e^2}{2M_e}\right)Nf \frac{1}{\epsilon_0} \left[ \frac{(\omega^2 - \omega_0^2)}{(\omega^2 - \omega_0^2)^2 + \omega^2\gamma^2} \right], \quad (2)$$

where  $e$  is the electron charge,  $M_e$  is the electron mass,  $N$  is the number density,  $f$  is the oscillator strength,  $\epsilon_0$  is the electric permittivity,  $\gamma$  is the linewidth,  $\omega$  is the radial frequency, and  $\omega_0$  is the resonant frequency. The authors' research group has developed a model for the real index of mercury vapor, including isotopes and hyperfine structure.<sup>7</sup> Variations in the derivative of the real index with respect to frequency cause variations in group velocity, or temporal dispersion. Narrow-band light of frequency  $\omega$  propagates through the vapor with a group velocity given by Eq. (1), whereas light much broader than the transition width propagates with nearly the unperturbed speed of light. The propagation delay time through a vapor cell for a seeded narrow-band pulse relative to an unseeded broadband pulse is then simply

$$T_{\text{delay}}(\omega) = \frac{L}{V_g(\omega)} - \frac{L}{c}, \quad (3)$$

where  $T_{\text{delay}}$  is the delay time and  $L$  is the cell length.

Figure 1(a) shows the modeled delay time of narrow-band light relative to broadband light as a function of frequency through a 5-cm-length mercury-vapor cell. Also shown is the modeled filter transmission, found from Beer's law. The complex structure is due to isotopic contributions as well as to hyperfine splitting. The frequency axis shown is relative to

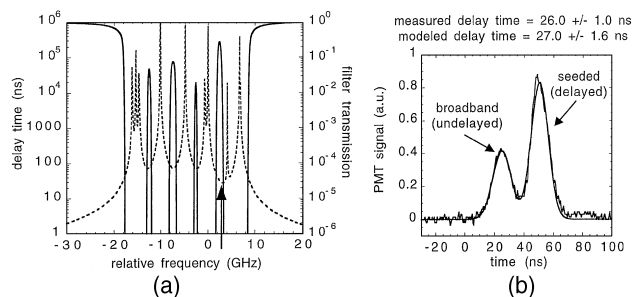


Fig. 1. (a) Modeled delay time (dashed curve) and modeled transmission (solid curve) for the 5-cm mercury-vapor filter near 253.7 nm. The multiple peaks are due to both isotopic abundance and hyperfine splitting. (b) Oscilloscope trace showing the narrow-band light delayed relative to the broadband light as well as a sum of two Gaussians fitted to the data. The laser frequency in (b) is marked by an arrow in (a).

$39412.4 \text{ cm}^{-1}$  (253.7 nm). The cell is modeled as having a vapor pressure of 0.445 Torr and a temperature of 403 K. The cell is an evacuated quartz tube of diameter 5 cm and length 5 cm. The vapor pressure is regulated by immersion of a cold tip containing liquid mercury into a temperature-regulated bath.

Figure 1(b) shows an oscilloscope trace that illustrates the GVD through the mercury filter. The early peak is due to the unseeded light; the delayed peak is due to the seeded pulse. The filter was operated as described above, and the laser was tuned as indicated in Fig. 1(a). Such traces were taken at a range of filter conditions and served to verify the GVD model; for example, in this case the modeled and measured delay times were  $27.0 \pm 1.6$  and  $26.0 \pm 1.0$  ns, respectively.

Separating the seeded and the unseeded pulses allowed us to measure the seeding efficiency of the third harmonic of our pulsed Ti:sapphire laser. The laser was injection seeded from a continuous-wave Ti:sapphire laser and operated with a ramp-and-lock feedback system to ensure single-mode output.<sup>8</sup> The output from the laser was attenuated significantly and then imaged through a mercury-vapor cell and collected with a photomultiplier tube (PMT; Hamamatsu Model R-960). The mercury-vapor filter was operated at conditions similar to those modeled in Fig. 1. A monochromator (ISA Model H20) was placed between the mercury filter and the PMT and was used to reject other colors of light from the pump beams and the first and second harmonics. We used boxcar integrators (Stanford Research Systems) to measure separately the integrated intensity of the unseeded (undelayed) light and the seeded (delayed) light. The unseeded light was measured with one channel, and a wider delayed gate from a second channel was used to measure the seeded light. The firing of the laser has some jitter, and care was taken to ensure that the unseeded signal did not overlap the delayed gate. Such a configuration ensured that all broadband light would appear in the first gate and that all light delayed by greater than  $\sim 25$  ns would appear in the second gate. Of course, for laser tunings for which the delays are less than  $\sim 25$  ns, the seeded light leaks into the first gate. Note that to see both the delayed

light and the undelayed light pulses simultaneously one must tune the laser to near the edge of the filter transmission, such that the filter absorption is comparable with the seeding efficiency ( $\sim 99\%$ ). In this case the seeded pulse is attenuated to a level comparable with that of the unseeded pulse, and the two pulses can be viewed at the same time.

Figure 2 shows the results of a frequency scan of the broadband and narrow-band signal amplitudes starting in the filter absorption and moving to the filter transmission. Also shown is the modeled narrow-band signal level. We established the frequency axis for the model by using data from a second, optically thinner, mercury-vapor filter, which acted as a frequency reference. The seeded signal is strongly absorbed within the notch and then becomes apparent as one moves toward the edge of the filter ( $I/I_0 \sim 0.01$ ). Meanwhile, the signal from the broadband light remains quite uniform, even in the spectral region where the seeded light is moving into the transmission, indicating that the linewidth of the broadband light is much wider than the filter ( $\sim 0.3 \text{ cm}^{-1}$ ). Tuning the monochromator indicates that the broadband light is narrow compared with the 3-nm passband of the monochromator, which allows us to bracket the linewidth of the broadband light by 0.3 and 300 wave numbers. In the filter transmission the seeded signal is undelayed, so both the seeded and the broadband signals appear in the first gate. To collect the signal in the filter transmission we inserted a neutral-density filter (transmission, 0.0056) into the beam path.

From such data it is straightforward to extract the seeding efficiency (or spectral purity), which we define as the fraction of seeded energy in the pulse. The signal measured with the laser tuned to the

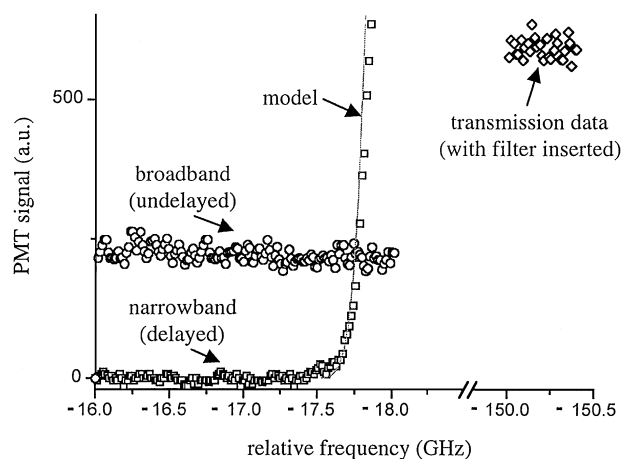


Fig. 2. Narrow-band (delayed) and broadband (undelayed) light intensities as the laser frequency is tuned from  $-16$  GHz (within the absorption notch) to  $-150$  GHz (far from the absorption). Within the absorption notch, the narrow-band component is strongly attenuated, and only the broadband component can be detected. The narrow-band (delayed) intensity agrees with the model (shown as a solid curve). Far from resonance, both components propagate through the filter with approximately the same speed and with no attenuation. The ratio of the broadband signal to the transmission signal measured far from resonance gives the seeding efficiency.

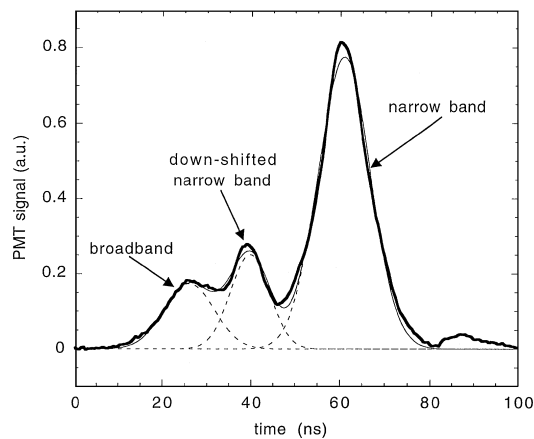


Fig. 3. Pulse chirping capability of the filter. The first (undelayed) peak of the oscilloscope trace is due to the broadband light, and the two delayed peaks are due to the two different frequency components (separated by  $\sim 2.3$  GHz) within the same pulse. Also shown are three Gaussian peaks and their sum fitted to the data.

filter transmission is due to both the seeded and the unseeded light. With the laser tuned inside the filter absorption, however, one may use the GVD to measure the broadband signal directly. Taking the ratio of these quantities gives the fraction of broadband energy in the pulse, or unity minus the seeding efficiency. To perform this measurement for a laser with high seeding efficiency generally requires insertion (or removal) of neutral-density filters because the broadband signal (measured in the absorption) is orders of magnitude less than the total signal in the transmission. If we normalize the transmission signal, with a 1/180 filter in place, to unity, then Fig. 2 will show an average broadband signal of 0.378. Thus we find that

$$\begin{aligned} \text{seeding efficiency} &= 1 - \text{fraction of broadband} \\ &\quad \text{light in pulse} \\ &= 1 - \text{broadband signal} \\ &\quad / \text{total transmission signal} \\ &= 0.998 \pm 0.0002. \end{aligned} \quad (4)$$

The uncertainty is found from the standard deviation of the data and reflects shot-to-shot variations. The seeding efficiency indicates that nearly all the light collected in the transmission is seeded. The tuning range of the fundamental (first harmonic) of the beam does not overlap the resonance of the mercury filter and therefore cannot be measured with the current setup. The seeding efficiency of the fundamental beam, or of other lasers, can be performed by exactly the same approach but by selection of an atomic vapor that overlaps their tuning range and offers sufficient GVD. For example, the fundamental of our laser could be measured with a rubidium filter at  $\sim 780$  nm.

A dual-frequency laser beam was used to demonstrate the pulse chirping capabilities of the vapor filter. The ability of the filter to chirp pulses in the nanosecond regime could be used for time-domain absorption or scattering measurements. Such measurements could be performed with standard nanosecond detectors and oscilloscopes and in a single shot. The

types of spectral width of interest would be those found in absorption or scattering line shapes, i.e., of the order of one to several gigahertz. To demonstrate the chirping capability, we use the filter to resolve temporally a pulse containing two distinct frequency components. Clearly, by superposition, the same approach could be used for a pulse with a continuum of frequency components. We used the downshifted light generated by Brillouin scattering in a high-pressure ( $\sim 40$ -atm)  $\text{CO}_2$  cell to introduce a second spectral component into the beam. By spatially overlapping a picked-off portion of the original beam with the downshifted beam we were able to generate a beam with two distinct frequency components as well as the residual broadband light. Path differences of the two legs were less than  $\sim 2$  cm, corresponding to negligible temporal differences ( $< 0.1$  ns). Figure 3 shows the oscilloscope trace generated by passage of the dual-frequency beam through the vapor filter. The laser is tuned close to the low-frequency edge of the absorption. Three contributions to the trace are visible: First, a pulse that is due to the undelayed broadband light appears; second, a pulse that is due to the downshifted light from the Brillouin scattering appears; and finally, a peak from the seeded, but unshifted, laser light is present. At this laser tuning, the downshifted beam is farther from resonance and therefore has a smaller delay time than the unshifted component.

We have demonstrated that the seeded and unseeded light within a laser pulse can be decoupled by use of the group-velocity dispersion in an atomic-vapor filter. For an atomic-vapor mercury filter the GVD and delay times have been accurately modeled in the spectral region near 253.7 nm. Discriminating between the narrow-band and the broadband components permits characterization of laser seeding, or spectral purity. Using this method, we measured the seeding efficiency of the third-harmonic output of our injection-seeded Ti:sapphire laser to be  $\sim 99.8\%$ . We also used GVD in the filter to demonstrate nanosecond pulse chirping, which may be used for time-domain spectroscopy.

A. P. Yalin's e-mail address is yalin@phoenix.princeton.edu.

## References

1. D. Hoffman, K.-U. Munch, and A. Leipertz, *Opt. Lett.* **21**, 525 (1996).
2. J. Altmann, R. Baumgart, and C. Weitkamp, *Appl. Opt.* **20**, 995 (1981).
3. D. Grischkowsy, *Phys. Rev. A* **7**, 2096 (1973).
4. A. Kasapi, G. Y. Yin, M. Jain, and S. E. Harris, *Phys. Rev. A* **53**, 4547 (1996).
5. D. L'Hermite, M. Comte, O. Gobert, and J. de Lamare, *Opt. Commun.* **155**, 270 (1998).
6. R. S. Longhurst, *Geometrical and Physical Optics* (Longman, London, 1967), p. 458.
7. N. D. Finkelstein, A. P. Yalin, W. R. Lempert, and R. B. Miles, *Opt. Lett.* **23**, 1615 (1998).
8. N. D. Finkelstein, W. R. Lempert, R. B. Miles, A. Finch, and G. Rines, AIAA Pap. **96-0301** (American Institute of Aeronautics and Astronautics, Washington, D.C., 1996).
9. R. W. Boyd, *Nonlinear Optics* (Academic, San Diego, Calif., 1992).